



Optimization of solid particle erosion behavior of thermally sprayed nichrome on duplex stainless steel

Roshan Kuruvila¹ · S. Thirumalai Kumaran² · Rendi Kurniawan³

Received: 3 December 2023 / Accepted: 3 April 2024

© The Author(s), under exclusive licence to Springer-Verlag France SAS, part of Springer Nature 2024

Abstract

Erosion stands as a formidable challenge within the industry, posing significant threats to pipeline integrity. This wear phenomenon occurs when minute solid particles collide with pipeline surfaces at specific angles and velocities. Given the pivotal role pipelines play in sectors like oil and industrial, their vulnerability to erosion wear presents a pressing concern. Solid particles inevitably accompany the fluids coursing through these conduits, subjecting them to erosion under harsh operational conditions. The repercussions extend beyond industrial realms, affecting both natural environments and societal well-being. Detecting and addressing erosion-induced damage promptly remains a daunting task, with potential leaks draining resources and disrupting operations. Unforeseen shutdowns further escalate operational costs and hinder productivity. Clearly, mitigating erosion wear is imperative for ensuring clean, safe, and efficient production processes. Consequently, industrial endeavors prioritize strategies to counteract erosion's deleterious effects. Technological advancements offer promising avenues for tackling this challenge. This investigation aims to devise effective solutions, focusing on the efficacy of a nickel–chromium erosion-resistant coating applied via atmospheric plasma spraying. A comprehensive analysis of erosion mechanisms and influencing parameters guides this endeavor. Through desirability analysis and Taguchi design of experiments, optimal parameters—flow velocity of 150 m/s, impact angle of 90°, discharge rate of 5 g/min, and 10 min duration—are identified. Notably, experimental results closely align with predictions, demonstrating a mere 3.03% variance.

Keywords Erosion · DGun coating · Taguchi analysis · Desirability

1 Introduction

The development of worldwide oil and gas sector in the second half of the twentieth century has increased demand for transport and the pathways that connect to the markets. Stainless steel pipes are among the most versatile and inexpensive modes of transportation available today [1]. The importance of pipelines is made apparent by the rapid development of the society and the increasing need of these fuels [2]. Pipelines are considered as being quick, cheap, simpler to operate, and

capable of transporting a lot more as compared to the traditional transportation devices. Pipelines are therefore the primary method of transport for oil and gas in the vast majority of the oil and gas industries around the world [3]. Transporting crude oil, natural gas, and refined petroleum products via pipelines is also the safest option. Despite many benefits of using pipelines for oil and gas transportation, such as faster, cheaper, and easier than the alternative methods, pipeline failures like leakage create significant problems for the global oil and gas industries [4]. The pipeline's ability to operate regularly is also threatened by the leakage incident, in addition to the environment and public safety [5]. As a result, this needs to be effectively managed.

Pipelines are vulnerable to leaks for a variety of reasons, including operating circumstances, environmental concerns, and human issues [6]. Erosion has been considered as a primary cause of oil and gas pipeline leakages. Erosion, a phenomenon that damages walls, due to the collision of solid particles carried out by fast-moving fluids [7]. Oil and gas production procedures usually involve the usage of fluids that

✉ S. Thirumalai Kumaran
thirumalaikumaran@yahoo.com

¹ Department of Mechanical Engineering, Amal Jyothi College of Engineering, Koovappally, Kerala 686518, India

² Department of Mechanical Engineering, PSG Institute of Technology and Applied Research, Coimbatore, Tamil Nadu 641062, India

³ Department of Mechanical Engineering, Faculty of Engineering, Universitas Indonesia, Kampus Baru UI, Depok 16424, Indonesia

are moving at high pressures and speeds while carrying solid particles. The accumulation of pipeline's fluid flow has the potential to reduce the wall thickness and perforates the pipe, both of which can result in leakages [8]. To mitigate the risk to society, the environment, and a safe working environment, the factors triggering erosion must be investigated.

This circumstance demonstrates the need to minimize excessive wear on pipes to ensure safe, clean production with improving efficiency. Thus, it would be perfect to carry out an in-depth investigation of all the variables influencing solid particle erosion in the oil and gas industry. This paper explores the effects of a wider range of parameters, including particle qualities, ambient circumstances, and material features, and integrates earlier research findings in the published literature. Hardness, shape, size, and density are the crucial characteristics of particles [9]. Environmental conditions include the environment's composition, temperature, time, slurry concentration, impact angle, and impact velocity. Strength, hardness, microstructure, and toughness are all the examples of material qualities [10]. Despite the fact that a number of mitigation strategies have been documented in the literature, the proposed study is focused on material choice and surface modifications. In the case of erosion damage in metals, mechanical and surface properties are significant [11]. Whether a specific attribute or a collection of related mechanical properties correlates with erosion resistance has been the subject of numerous investigations. As hardness shows the resistance of a metal's surface to plastic deformation and has been effectively associated with the metal's resistance to wear phenomena, it has attracted a great deal of attention. Moreover, Heymann [12] explained how hardness and erosion rate are related. Recent research demonstrating the resistance to erosion of stainless steel has validated this interpretation [13]. Erosion poses a problem for the oil and gas producing sector. Every phase of the design, establishment, and operation of pipe systems and their accessories necessitates careful consideration of material selection. Consequently, these components require exceptionally high mechanical properties as well as exceptional erosive resistance from the materials used to make them. Duplex stainless steels (DSS) are widely used due to their superior mechanical characteristics. DSS is more flexible and durable than other types of stainless steel. Due to their lower nickel content, duplex stainless steels have cost-saving benefits in addition to the aforementioned qualities. DSS, have nearly equal amounts of austenitic and ferritic structure [14, 15]. Bain and Griffiths initially characterized the duplex steel in 1927, but they were not commercially available until 1930s. Later, DSS 2205 was developed and employed as the foundation for the emergence of the contemporary steel family. Subsequently this has grown with significance and they are now recognized as workhorse materials in numerous applications. They are extensively utilized

in civil and structural engineering, pulp and paper, maritime, chemical processes, oil and gas, and power industries [16]. Due to their minimal maintenance requirements in severe conditions, DSS have replaced carbon steel in a variety of applications. Due to their great strength, duplex stainless steels may be thinner and more cost-effective throughout the course of their lifetime compared to other carbon steels [17].

The selection of materials is not adequate to prevent failure or unfavorable maintenance costs as some materials may not hold up well in harsh situations. Research proved that erosion can be reduced or even completely eliminated by using surface modification techniques [18]. Coatings are crucial in industrial applications as they reduce surface degradation and improve the tribological performance of materials. Surface coatings have a major impact on mechanical properties including hardness, strength, and toughness. Tailored coatings also enhance mechanical capabilities by combining different materials with complementing properties. Understanding coating-substrate compatibility, endurance, and cost-effectiveness is essential to customizing coatings for specific purposes and ensuring the successful application of coatings in industrial applications [19]. The use of various thermal spray coatings methods, such as high velocity oxy fuel (HVOF), detonation gun coating (DGun) and atmospheric plasma spray (APS) are the state-of-the-art for coating components which are vulnerable to erosion. The coatings created by thermal-spraying processes have many benefits, including the ability to protect equipment and structures, provide a cosmetic finish, modify the chemical, mechanical, and thermal properties of materials, and increase the efficiency as well as wear resistance of components when applied to low-cost substrates. They also act as a barrier between the substrate and the harsh marine or industrial environment.

The thermal spray coating procedure, which gives exceptional surface resistance to erosion, is an additional method to prevent or mitigate erosion. Thermal spray coating has been used to achieve up to 16 times higher erosion resistance [20]. Thermal spray coating's use and application have increased, due to the improvement of various erosion-resistant characteristics [21]. Since they are the most adaptable and employed to coat various materials and associated combinations [22], thermal spray coating techniques like DGun techniques are commonly used. Kamal et al. [23] have used a special DGun coating technology known for creating coatings with solid, compact microstructures and minimal porosity. Due to its faster speed and lower operating temperatures, coatings will provide strong adherence as well as the liberty to change the depositing settings to achieve appropriate surface properties. Detonation spraying has been preferred by Bolelli et al. [24] over plasma spraying and other spraying techniques. A coated surface produced by the DGun spray process, a thermal spray coating technique, has compressive residual

stresses, very low porosity, and an incredibly high adhesive strength [25]. It was established that thermal spraying is the best technique to generate an array of coatings that increase the functionality and lifetime of engineering components subjected to various types of wear. An appropriate thickness can be produced on the work piece by controlling the combustion gas ratio, powder particle size, carrier gas flow rate, frequency, and distance between the barrel end and the substrate.

Coating ceramics, metallic alloys, polymers, elastomers, and composites may provide a variety of materials with the desirable features to produce erosion-free surfaces. The resistance to erosion is enhanced, when the substrate is coated with nichrome (NiCr) through appropriate deposition techniques. According to the research done by Swaminathan et al. [26], it can provide materials with higher hardness and lower porosity. Li et al. [27] claimed that when the substrate is exposed, the NiCr coating resists deterioration more effectively. The NiCr based coating has also been shown by Kawahara [28] to offer increased resistance to oxidation, wear, and corrosion, making it appropriate for a variety of applications. Further research done by Behera et al. [29] has suggested that NiCr coatings can enhance erosion resistance. According to the investigations by Abyazi and Kiyani [30], NiCr coatings can increase erosion resistance in solid particle erosion situations. A careful review of the literature thus draws the conclusion that NiCr coatings are able to resist erosion wear in challenging circumstances.

The erosive wear of components brought on by abrasive particles is a significant technological challenge. Since the operating requirements in challenging environments are the main causes of erosive wear, understanding the solid particle erosion characteristics is critical. More researches are required to determine the significance of cermet coating in this field from both scientific and commercial perspectives. The development of materials in a way that would minimize or control wear also requires a thorough understanding of all the factors that influence erosive wear. As defined by Davis [31], wear is the degradation of a substance caused by the collision of fast-moving particles. As quoted by Hutchings [32], erosive wear is a type of wear caused by hard particles. The term “erosion” describes wear that happens when a flowing liquid or gas forces hard particles to the surface of a material. More damage could be done by liquid jets or droplets that come in contact with the surface. Solid particle erosion is the gradual loss of material from a component’s surface, due to rapidly moving hard elements, as defined by Davis [33, 34].

Erosion may prove challenging to deal with. It has a complex nature as a result of an array of impacting elements. The subject material and its erodent, which move through the flowing fluid at an identified velocity, are the main components of the erosion process [35]. Investigations of Sun

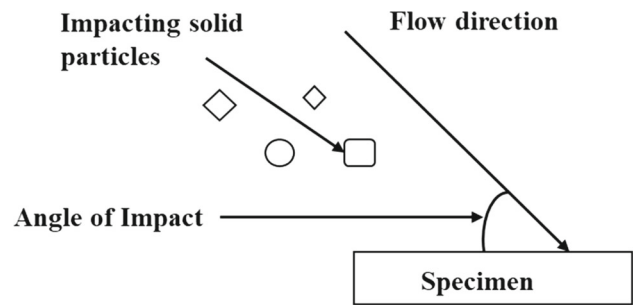


Fig. 1 Schematic diagram for angle of impact

et al. [36], Alqallaf and Teixeira [37], and Hu et al. [38] have examined how particle factors and a material’s physical properties affect erosion rate.

The environment, target materials, and impact particle velocity all generally have a significant impact on the erosion mechanism [39]. In pipelines used for the transportation of gas and oil, they are often carried at specific velocities. Increasing the product’s velocity may increase the impact velocity of the solid particles striking the steel surface. The erosion process that degrades the pipeline surface can also be impacted by impact velocity. Localized plastic strain during erosion in the oil and gas industry surface has been established as a result of solid particle bombardment on the steel surface [40]. Increasing the impact velocity can increase the surface roughness of the steel as well as the erosion rate.

The impact angle, as shown in Fig. 1 which is one of the elements, has the greatest impact on erosion, as reported by Singh et al. [41]. The fundamental concept in the angle of impact on the pipeline surface is that when metals come into contact with hard particles in the fluid, the protective oxide covering on the metal surface ruptures or is removed. More severe surface deterioration follows as a result of the solid particles’ continual bombardment of the exposed surface at various contact angles with the moving fluid. However, the surface material determines how it influences erosion. The majority of materials utilized in the oil and gas sector exhibit both brittle and ductile properties.

As the particles’ impact velocity depends on the carrier flow velocity, the size of the erodent is one of several factors contributing to erosion. Studies revealed that, up to a particular size (50–1000 μm), particle size has a major impact on the erosion rate. It was suggested that the erosion rate would become independent of particle size beyond this range of values [42]. Numerous investigations have looked into how particle shapes and sizes affect erosion. It was demonstrated that on the impinging surface, sharp abrasive particles remove more material than spherical ones. Additionally, it was observed that four times as much erosion can be caused by angular particles as by spherical ones [43].

Experiments with particles of various sizes by Lynn et al. [44] and Clark and Hartwich [45] have revealed that the efficiency of particle collision decreases with increasing particle size. According to Turenne et al. [46], there is a correlation between erosion efficiency and sand concentration. An increase in concentration would result in more particles rebounding and shielding the surface from approaching particles. Tewari et al. [47] have studied the erosion's response to exposure time and found that it linearly increases before reaching a stable state. The combined impact of various factors on solid particle erosion has been studied by Balamurugan et al. [48] and Kuruvila et al. [49]. The relative contributions of each element have been examined, and the recommendations for reducing the erosion rate have been taken into consideration.

It becomes apparent that these characteristics significantly influence erosion rate. On the basis of variance analysis, the key factors influencing the responses have been identified [50, 51]. Combinations of these optimized influential parameters are employed to effectively control erosion. The experiments have been designed using Taguchi's orthogonal technique, which is based on the experimental investigations of Benterki et al. [52], Choudhary et al. [53], and Kuruvila et al. [54]. This method has identified the ideal combination of control parameters for the erosion process and it minimizes the erosion rate. Experiments are designed and performed according to L_{27} Taguchi experimental design to analyze the role of controlled parameters on the overall erosion process. Finally, recommendations have been given based on the S/N ratio graph results under various operating conditions of the experiment.

The present research focuses on the positive effects of NiCr surface coating on DSS 2205 substrates and investigates the potential applications for these coatings on oil and gas pipelines. DSS exhibit impressive mechanical properties and erosion resistance in hostile settings, but there are few investigations on the erosion behavior of DSS coated with NiCr. More investigation is still needed to fully comprehend how different factors impact erosion on duplex stainless steel with NiCr coating. The literature's investigation of erosion optimization is not comprehensive enough. The proposed study is predicated on this concept.

2 Experimental setup

2.1 Materials

DSS 2205 is selected as the substrate, due to its exceptional characteristics. High erosion resistance and strength materials are necessary in the oil and gas exploration and processing industries due to the harsh environmental conditions. The microstructure of DSS is made up of 50% ferrite and 50%

Table 1 (a). Mechanical properties of DSS 2205. (b). Physical properties of DSS 2205

Tensile strength	Yield strength	Elongation	Hardness
(a)			
621 Mpa	448 Mpa	25%	31 HRC
Density	Elastic modulus	Thermal conductivity	Electrical resistivity
(b)			
7800 kg/m ³	190 GPa	19 W/m.k	850 m-ohm.meter

Table 2 (a). Mechanical properties of NiCr. (b). Physical properties of NiCr

Tensile strength	Yield strength	Youngs modulus	Hardness
(a)			
330 Mpa	275 Mpa	150 MPa	37.6 HRC
Density	Elastic modulus	Thermal conductivity	Electrical resistivity
(b)			
8650 kg/m ³	170 GPa	8 W/m.k	84 m-ohm.meter

austenite phases, which has replaced the position of stainless steel in oil and gas installations. The benefits of both the austenite and ferrite phases were merged to create DSS, which is more corrosion- and erosion-resistant than austenitic stainless steel. Since DSS addresses ordinary pipe issues with performance and meets stringent environmental standards for oil and gas extraction and transportation, it offers a wide range of application potential in this industry. Samples with the dimensions of 25 mm × 25 mm × 5 mm are cut from the sheets of the work piece material using abrasive water jets. Mechanical and physical properties of DSS 2205 is shown in Table 1a, b.

Alloys based on nickel constitute is important in any thermal spray industry. These materials are frequently employed as surface coatings in many applications where a combination of qualities, such as strong wear resistance, and simultaneous erosion-corrosion resistance, are required. When chromium oxides to Cr₂O₃, the NiCr alloy forms a thin layer of protective chromia that renders it appropriate for erosion resistance. As a result, they effectively shield the surface from severe erosion and degradation. Hence NiCr is used in this study. Table 2a, b shows the properties of NiCr powder. Figure 2 exhibits the spherical form of the powder as seen in the SEM images. Using EDAX images (Fig. 3), the chemical composition of the powder is confirmed. Before depositing the

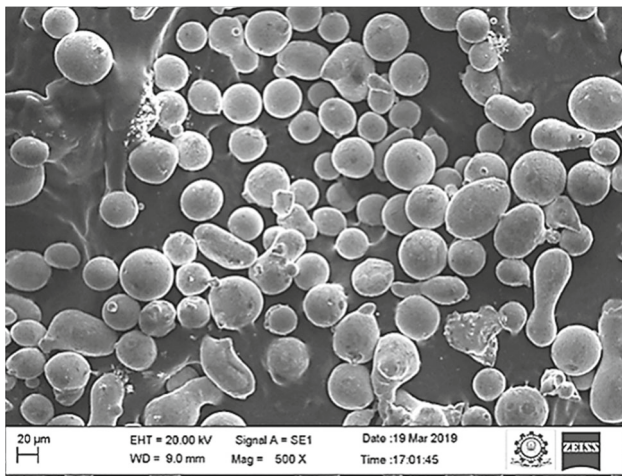


Fig. 2 Morphology of NiCr powder

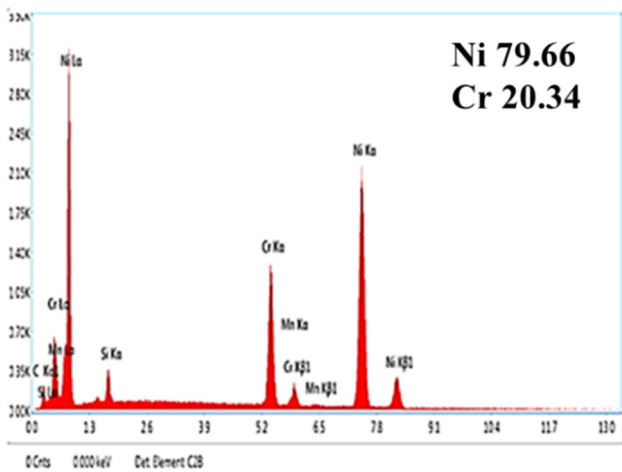


Fig. 3 EDX image of NiCr powder

coating, any moisture that remains in the powder is heated and dried.

2.2 Thermal spray coating

The specimens are subjected to thermal spray coating namely DGun method which was carried out at Sai Surface Coating Technologies, Hyderabad, India. The DGun coating condition is as follows: oxygen flow = $10.3 \times 10^{-3} \text{ m}^3/\text{s}$, fuel flow = $0.03 \times 10^{-3} \text{ m}^3/\text{s}$, argon flow = $0.013 \times 10^{-3} \text{ m}^3/\text{s}$, powder rate = 40 g/min and spray distance = 170 mm. Multiple coating deposition runs is used to develop the coating for the desired thickness. Prior to the creation of coating, the coatability and the methodical process factor optimization are accomplished. Coating with a minimum thickness of 100 μm is placed on the substrate faces, and the number of passes is modified as a response.

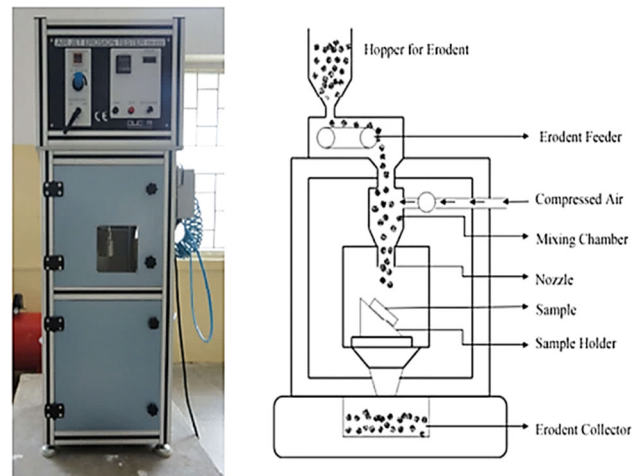


Fig. 4 Erosion Test Rig

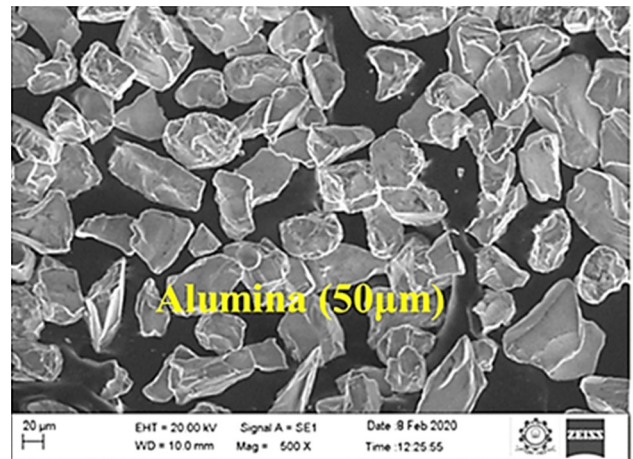


Fig. 5 Erodent particle

2.3 Erosion test

The erosion behavior of each experiment sample was investigated using an air jet erosion testing machine (TR 470, Ducom, Bangalore, India) in accordance with ASTM G76. The schematic diagram of air jet erosion test rig is shown in Fig. 4. The room temperature (30 °C), humidity (35%) and other testing variables are maintained as constant. Alterations are made to the impingement angle, flow velocity, time and discharge rate in order to evaluate the erosion behavior of every specimen and the erosion rates are estimated. 50 μm sized alumina oxide particles are used as the erodent. Figure 5 shows the erodent particle's morphology. The parameters used to conduct the erosion test and the analysis is listed in Table 3.

The erosion test was performed at room temperature. The change in mass during the erosion test is the primary variable that affects the erosion rate. As a result, the samples are

Table 3 Erosion test parameters

Factors	Level 1	Level 2	Level 3
Flow velocity (m/s) (A)	150	175	200
Impact angle (deg) (B)	30	60	90
Discharge rate (g/min) (C)	2.5	3.75	5
Test time (min) (D)	10	20	30

cleaned with acetone, dried, and weighed with an accuracy of ± 0.01 mg on an electronic scale. The erosion rate (E_r) is calculated by using Eq. (1).

$$\text{Erosion rate } (E_r) = \frac{W_i - W_f}{(E_f \times t)} \quad (1)$$

where, W_i = weight of the specimen before erosion (g), W_f = weight of the specimen after erosion (g), E_f = discharge rate (g/min), t = discharge duration (s).

2.4 Design of experiment

Statistically organized research studies by factorial methods reduce the costs and provide information and primary effects on the response parameters. The number of experimental trials is exponentially high in full factorial designs and it results in significant cost and time. In order to balance the cost and result accuracy, researchers frequently choose fractional factorial designs for their experiments. Orthogonal arrays based on Taguchi technique and response surface methods are employed in the current work to create the experimental matrix because they offer a cohesive combination of parameters with low number of trial-and-error iterations. Two

tests are carried out and the mean response values are used for the analysis.

3 Results and discussions

3.1 Microstructure analysis

Figure 6a, b displays SEM images of the surface and the cross-sectional view of the coating on the DSS 2205 substrate. The micrographs indicate exceptional adhesion at the interface and no marks of delamination. No cracks could be seen in the coatings, which have an average coating thickness of $100 \mu\text{m}$. Intersplat boundaries, porosity, voids, and other characteristics of the typical microstructure of coating can be seen. Coatings have a thick, consistent microstructure and high cross adhesion. The greater particle velocities attained by the detonation spray method result in improved cross-binding and less visible splat borders.

3.2 Erosion test

Erosion behaves with nonlinear processes with reference to its variables, materials and operating environments. To obtain the best solution to the erosion problem, the right combinations of operating parameters are to be ensured. The effect of variables on erosion may differ depending on the working environment. Figure 7 shows how the impact angle influences the rate of erosion at different velocities of erosion. The highest degree of deterioration happens at a 30° impact angle. As the impact angle increases, the erosion rate gradually declines. The erodent velocity has a significant effect on the erosion rate at various impact angles. The surface

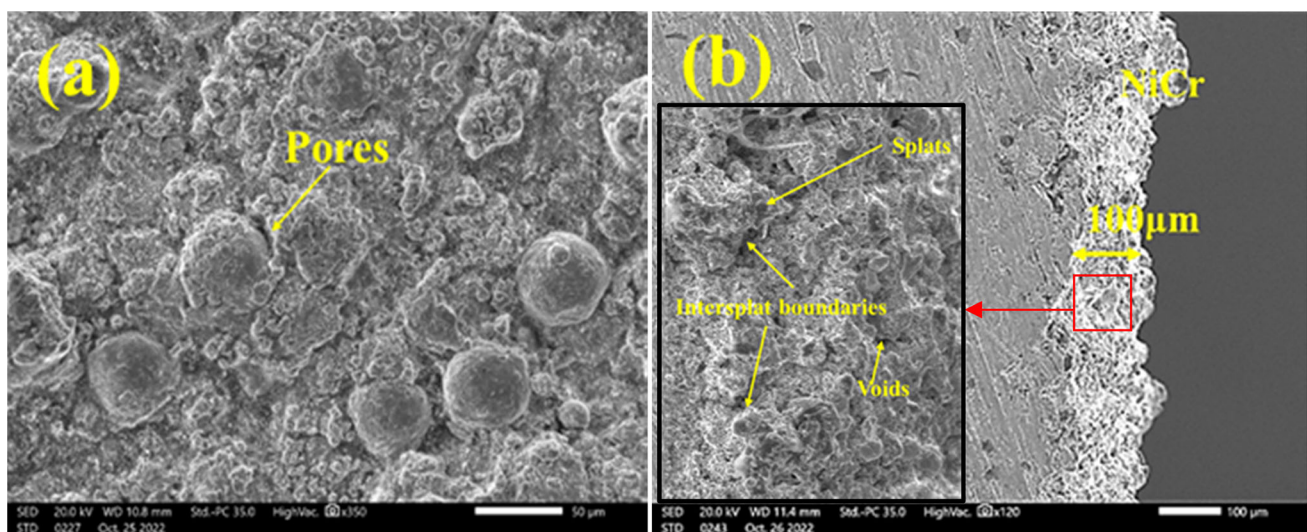


Fig. 6 SEM image **a** coated surface, **b** coating thickness

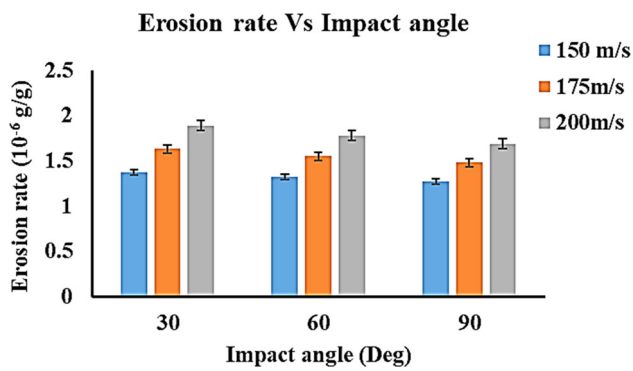


Fig. 7 Effect of impact angle on erosion rate at different flow velocity

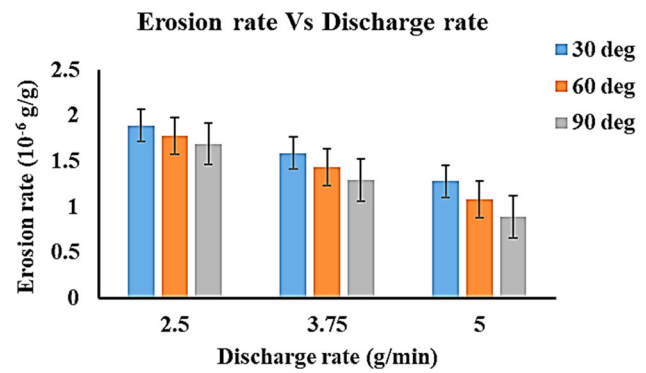


Fig. 9 Effect of discharge rate on erosion rate at different impact angles

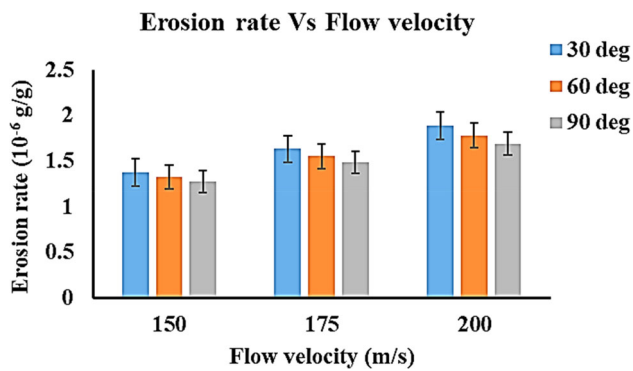


Fig. 8 Effect of flow velocity on erosion rate at different impact angles

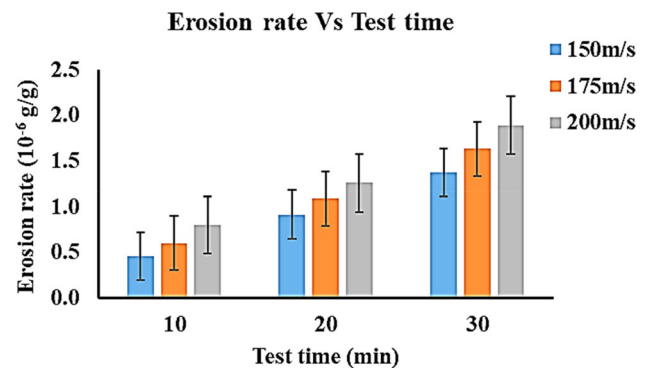


Fig. 10 Effect of test time on erosion rate at different flow velocities

undergoes strain hardening as a result of the repeated impacts results in plastic deformation. The connecting of the micro fractures triggers the material removal. Lower impact angles produce a completely different wear mechanism when compared to 90° . The likelihood of material removal increases with repeated ploughing in the same area. These factors led to the highest erosion rate at lower impact angles. The surface area exposed to erosion at 30° is greater than the surface area exposed at 90° , which is another crucial factor. Lower impact angles lead to more diverging of the particle and air mixture and it extends the erosion area [55].

Figure 8 shows how erodent velocity impacts erosion rate. The erosion rate is observed to be substantially impacted by erodent velocity in several pieces of literature. The increase in particle kinetic energy with increasing velocity causes significant damage to the surface [56]. The highest amount of material is removed, when the erodent particle impacts repeatedly, accelerating the erosion rate in return.

The correlation between the erosion rate and the erodent discharge rate is depicted in Fig. 9. When the erodent particle discharge rate is increased, it is found that the erosion rate decreases. The quantity of erodent striking the surface decreases with higher discharge rates. Additionally, the erodent impact time is reduced. The rebounding particles provide a shielding effect to the incoming particles and it

causes deviation in the trajectory of the incoming particles [57]. These factors have contributed to the increased erosion rate at higher discharge rates.

Figure 10 displays the relationship between the erosion rate variation and the test duration. When the test duration is increased, it is observed that the erosion rate increases. The quantity of erodents striking the surface increases with time. Additionally, the duration of the impact lasts longer. These factors have contributed to a higher erosion rate at extended test duration.

In accordance with the information, the highest erosion rate happens during shorter test duration at higher velocities, lower impact angles, and lower discharge. The fundamental cause of the phenomenon is that at lower impact angles, there is a minimal particle rebounding as the erodent, which comes after an impact, moves easily across the surface of the material and accumulates as debris. While at higher impact angles, it limits the progressing erodents and causes collision, which prevents from hitting the surface.

The sharp edges of the erodent strike the surface with high kinetic energy at a lower impact angle. It ploughs through the surface of the material and slips over it at this high speed. These surfaces are identified by more erodent ploughing in the direction of the erodent attack. The exposed surface

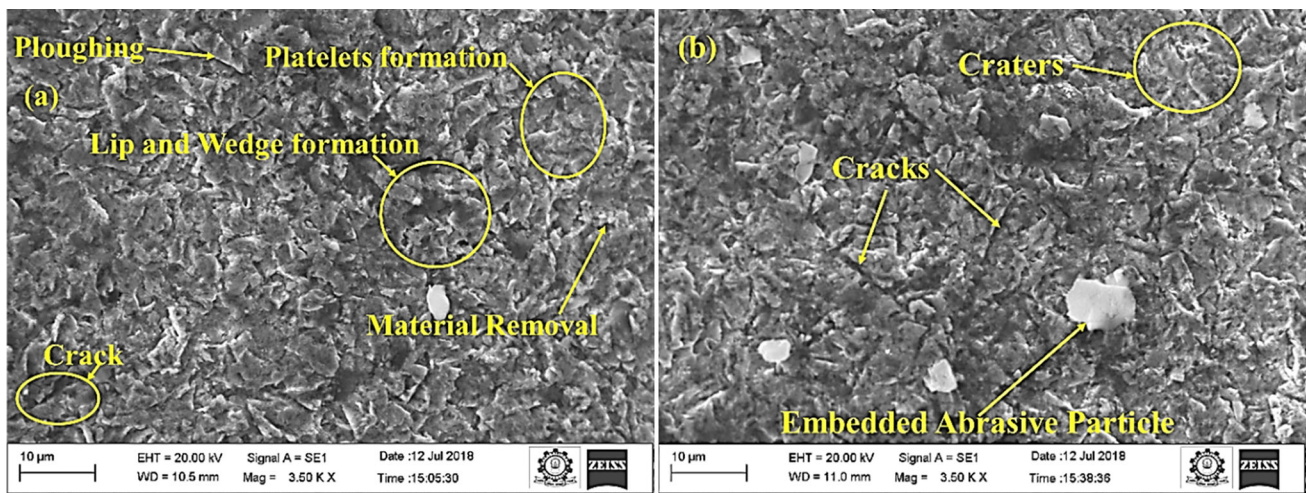


Fig. 11 SEM images of eroded surface **a** maximum erosion **b** minimum erosion

experiences increased strain rates, as erodent particles continuously impact. The wedge and lip creation on the surface is a result of the continuous attack. The wedge structure is broken into tiny platelets, due to the erodent's repeated attacks on the lips. A few cuts are also seen on ploughed surface. The outer layer becomes weaker, due to the erodent particle's frequent attacks. It also results in material separation at the surface and the erosion wear [48].

Higher impact angles lead to minimum erosion, which is accompanied by strain hardening on the eroded surface, due to continuous attack by erodent particles and the development of craters as shown in Fig. 11. There is the risk that the material around the produced cracks could delaminate, when these cracks branch out and are joined to the adjacent crack [58]. The propagation of microcracks triggers the growth of macrocracks, which cause the material to spallate [59].

3.3 Erosion mechanism

After analyzing the eroded specimens to understand the erosive wear mechanism at different impact angles, SEM images were obtained. The tangential component of the striking particles' kinetic energy was used by micro-cutting on the ploughed surface at low impact angle (30°), and its value was greater than the normal component, which was consumed by penetrating the surface. The metal's plastic actions along the flow direction on the eroded surface created the narrow cracks. On surfaces that were primarily the accumulation of metal brought on by particle extrusion, the lips are visible. These fragile lips may break easily as more particles impact them [60].

The number of cracks in the eroded area decreased as the impact angle increased to 90° , and the particles' sliding distance on the specimens' surface gradually decreased too.

Higher impact angles were found to cause stronger indentations, especially in the case of the indentation craters created by the direct impact of particles throughout the entire erosion range. In this type of erosion, metal accumulation in the form of ridges may occur around the indentation craters as a result of the striking particles' repeated extrusion. The collected metal tended to develop micro cracks under continuous particle contact. These fractures could eventually grow and unite to produce flake-like debris, or they could fall off during successive particle impacts [61]. The primary mechanisms of erosion at a 30° impingement angle are micro-ploughing and micro-cutting; at a 90° impingement angle, the predominant mechanisms are deformed platelets.

In addition to impact angle, flow velocity plays an important part in determining the degree of erosion at various impacts [62]. At higher flow velocities, the particles possess greater kinetic energy before they strike. Particles having a faster flow velocity therefore penetrate through the specimen surface, resulting in deeper penetration and a longer sliding distance. The obvious thing to observe was that particles with higher flow velocities generated longer and deeper cracks. The investigation of the erosion mechanism of eroded surface morphology under flow velocity effect led to the conclusion that pipelines operating in high-pressure, high-flow rate conditions are more susceptible to severe erosive wear.

3.4 Taguchi analysis

The Taguchi analysis is performed for the experimental results. Using MINITAB 18®, the experimental result is translated into signal-to-noise (S/N) ratios using the lower-the-better quality criteria. The S/N ratio difference indicates which parameter has the most impact. The response is used to analyse the impact of four erosion control parameters on the erosion rate, as shown in Table 4. The difference between the

Table 4 Experimental output and S/N ratio

Expt no	Flow velocity (m/s)	Angle of impact (deg)	Discharge rate (g/min)	Time (min)	Erosion rate (10^{-6} g/g)	S/N ratio
1	150	30	2.5	10	0.32	9.90
2	150	60	2.5	10	0.28	11.06
3	150	90	2.5	10	0.23	12.77
4	150	30	3.75	20	0.60	4.50
5	150	60	3.75	20	0.49	6.13
6	150	90	3.75	20	0.43	7.32
7	150	30	5	30	0.82	1.72
8	150	60	5	30	0.64	3.88
9	150	90	5	30	0.53	5.51
10	175	30	3.75	30	1.05	- 0.44
11	175	60	3.75	30	0.92	0.75
12	175	90	3.75	30	0.76	2.41
13	175	30	5	10	0.28	11.04
14	175	60	5	10	0.26	11.72
15	175	90	5	10	0.19	14.40
16	175	30	2.5	20	0.74	2.60
17	175	60	2.5	20	0.61	4.23
18	175	90	2.5	20	0.56	5.08
19	200	30	5	20	0.67	3.54
20	200	60	5	20	0.58	4.79
21	200	90	5	20	0.47	6.58
22	200	30	2.5	30	1.27	- 2.08
23	200	60	2.5	30	1.02	- 0.17
24	200	90	2.5	30	0.94	0.54
25	200	30	3.75	10	0.35	9.17
26	200	60	3.75	10	0.29	10.81
27	200	90	3.75	10	0.25	11.97

maximum and minimum mean value of S/N ratio provides the value of delta of the associated factor in the response table. Greater the delta value, the more significant the response characteristics. Depending on the significance of the output results, the components are ranked in ascending order.

The mean effect of S/N ratios on erosion rate formation is shown in Fig. 12. As the test duration and flow velocity decreases, the erosion rate increases. Whereas the impact angle and the discharge rate increase, the erosion rate decreases. This further illustrates the tendency of erosion rate. Due to close S/N ratio values, it is highly challenging to identify the parameter with the most influence from the mean effect plots. In order to determine the most affecting element as well as the correlation between different characteristics, more study is required. 150 m/s of flow velocity (A1), 90° impact angle (B3), 5 g/min of discharge rate (C3), and 10 min of duration (D1) have been identified to be the

optimal combination of factors for minimizing the rate of erosion.

Table 5 indicates how various S/N ratios respond to the rate of erosion. The delta values for each factors are shown in response table. The rank of a particular variable is represented by higher value of delta. The calculated data indicate that among the process parameters, time has the highest rank. It is relatively simple to calculate the optimum testing conditions for these control elements from the response table.

The interaction plot indicates how the erosion parameters interact with one another as shown in Fig. 13. Depending on the parametric interaction, lines may appear parallel or nonparallel. Parallel lines show no link between the parameters whereas intersections show some interaction between the parameters [63]. The statistical importance of experimental factors which include impact angle, velocity, test duration, and discharge rate was established by performing an analysis of variance (ANOVA) experimentation on the

Fig. 12 Main effect plot for S/N ratios of erosion

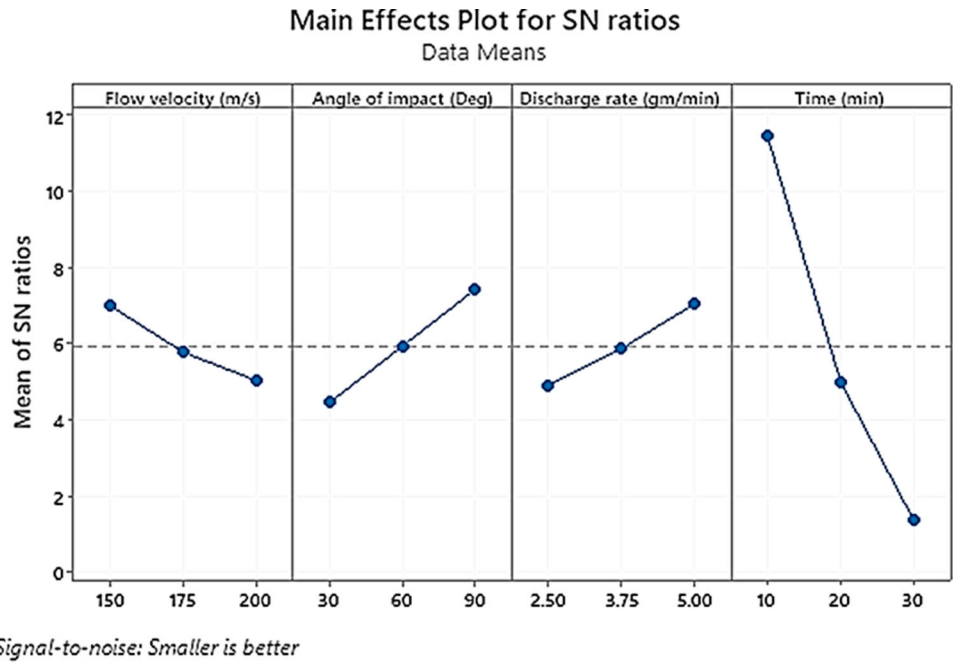


Fig. 13 Interaction plot for erosion

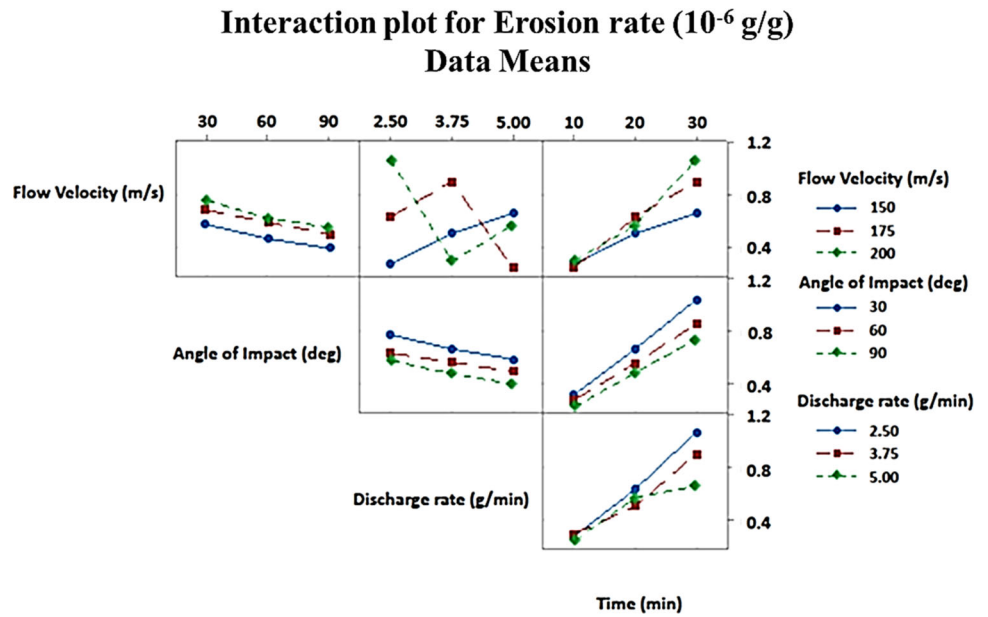


Table 5 Response table for S/N ratio (smaller-the-better)

Level	Flow velocity (m/s)	Angle of impact (deg)	Discharge rate (g/min)	Time (min)
1	0.4822	0.6769	0.6636	0.2721
2	0.5967	0.5655	0.5706	0.5714
3	0.6476	0.4841	0.4923	0.8831
Delta	0.1653	0.1929	0.1714	0.6110
Rank	4	2	3	1

Table 6 ANOVA for erosion rate

Source	DF	Seq SS	Adj SS	Adj MS	F	P	% of contribution
Flow velocity (m/s)	2	17.612	17.612	8.806	60.03	0.000	3.2
Angle of impact (deg)	2	39.367	39.367	19.683	134.18	0.000	7.16
Discharge rate (g/min)	2	20.687	20.687	10.343	70.51	0.000	3.78
Time (min)	2	469.108	469.108	234.554	1598.94	0.000	85.38
Residual Error	18	2.640	2.640	0.147			0.48
Total	26	549.415					100%

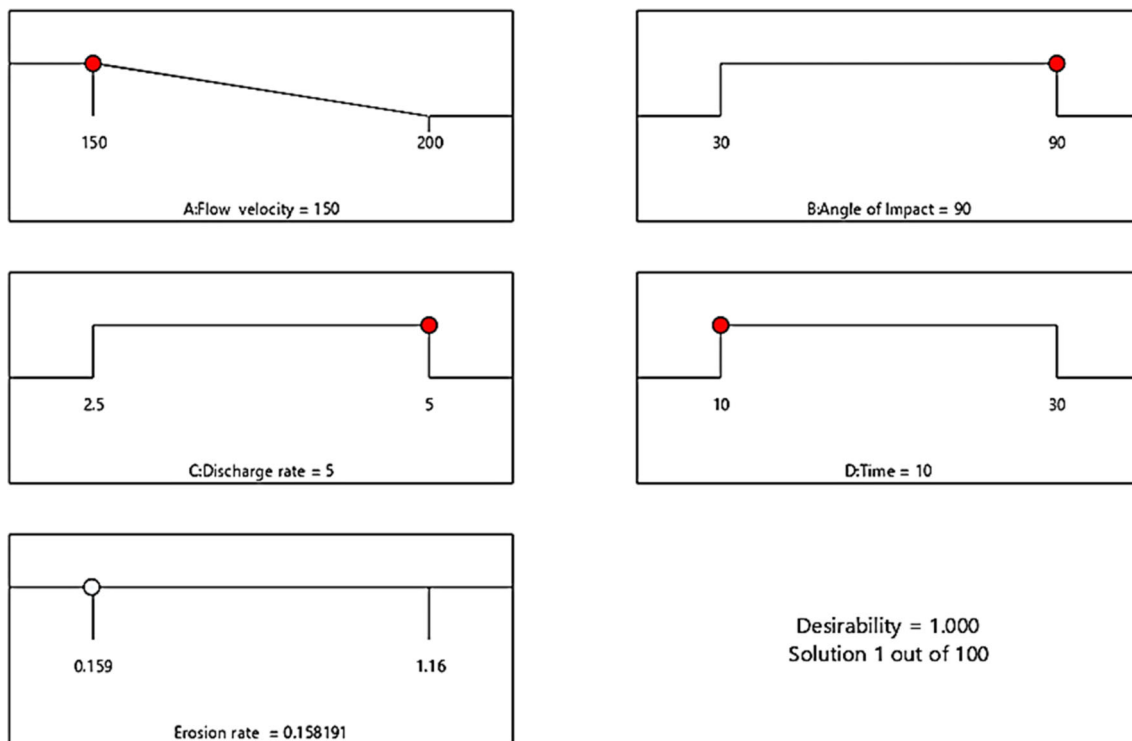


Fig. 14 Ramp function graph of desirability

investigational results. A higher correlation coefficient (R^2) value indicates how well the predicted model fits the observed data. The current percentage, 99.52%, demonstrates how well the researched models fit the findings of the experiment [64]. Table 6 exhibits the percentage contribution of each element to the erosion rate.

3.5 Regression analysis

The rate of coated DSS 2205 erosion is modeled using linear regression analysis. As indicated in Eq. (2), it can be expressed as erosion rate, as a function of various factors. The R^2 in the regression model is obtained as 0.96. The developed model and the experimental erosion rates are thus nearly

identical in agreement.

$$\begin{aligned}
 \text{Erosion rate } (10^{-6} \text{ g/g}) &= -0.164 + 0.003307 \text{ flow velocity} \\
 &\quad - 0.003214 \text{ angle of impact} \\
 &\quad - 0.0685 \text{ discharge rate} + 0.03055 \text{ Time} \quad (2)
 \end{aligned}$$

Considering its widespread usage in developing suitable approximation methods, the Desirability analysis is employed to predict the correlation between the input parameters and the output variables with the minimum number of experiments [65]. This methodology can be used when a process’s quality characteristic or performance indicator

is influenced by a large number of input variables. Design Expert software is used to create this RSM-based experimental investigation, which is organized in accordance with RSM's central composite design (CCD). All other parameters are held constant during the experimentation. In order to minimize the erosion rate, the parameters are optimized by utilizing desirability-based response optimization approaches. The desired result obtained is 1.00, as shown in Fig. 14. The desirability prediction perfectly matches with the Taguchi estimates, confirming that the optimal condition is achieved.

A perturbation plot (Fig. 15) shows how the response changes when one factor deviates from the selected reference point while the other factors remain constant at the reference point. The reference point, or the coded zero level of each factor, is frequently set by default by the Design-Expert program at the centre of the design space. It is observed when the flow velocity changes, the erosion rate has an increasing influence. The illustration also makes it clear that the erosion rate increases with the decreasing discharge rate and the erosion rate reduces with the increasing angle of impact.

In the predicted versus actual plot, the data almost perfectly form a straight line, suggesting a close relationship between the actual and the predicted results. The plot's predicted and the actual erosion rates are displayed in Fig. 16. It is observed that the fit is insignificant [66].

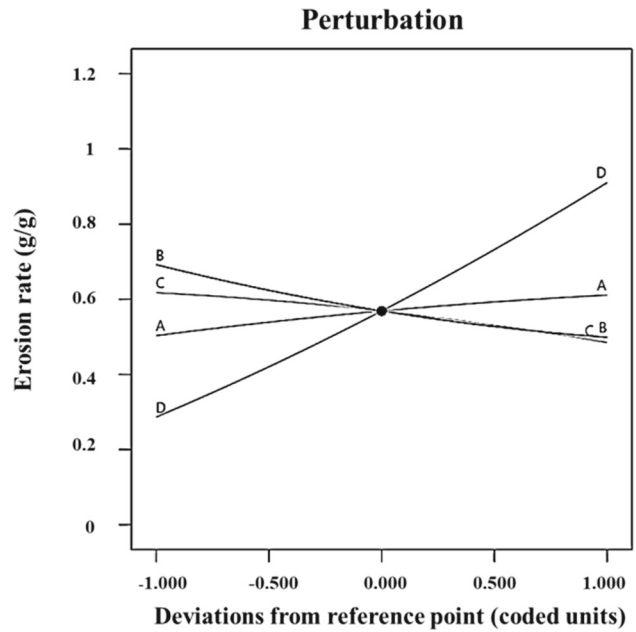


Fig. 15 Perturbation plot

3.6 Confirmation test

The specimens were tested at the optimal parameter settings for the confirmation test: impingement angle = 90°, velocity = 150 m/s, discharge rate = 5 g/min, and test time = 10 min. The conclusions of the erosion rate confirmation test are shown in Table 7. The error difference between the experimental and confirmation test values was only 3.03%. Hence the model confirms the significance.

Fig. 16 Predicted versus actual plot

Erosion rate

Color points by value of erosion rate

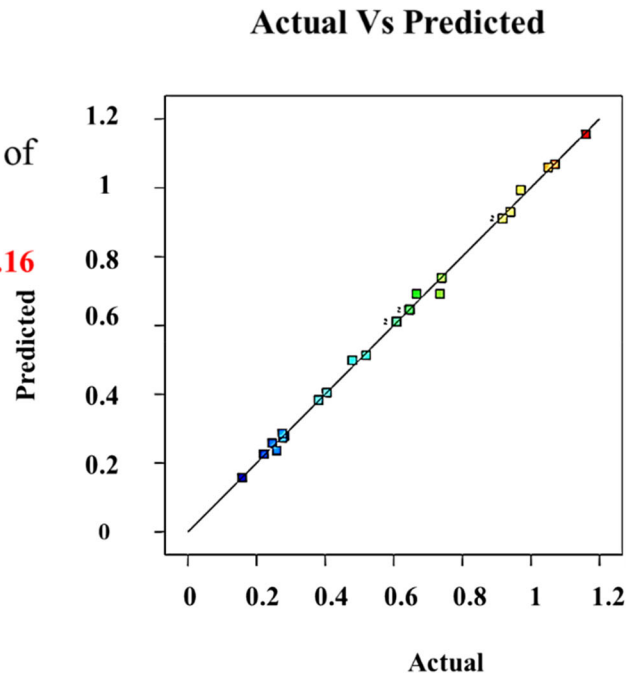
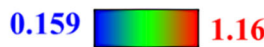


Table 7 Confirmation results

Optimal condition		Erosion rate (10^{-6} g/min)	Error (%)
Flow Velocity = 150 m/s	Experimental	0.1629	3.03
Angle of Impact = 90°	Predicted	0.1582	
Discharge rate = 5 g/min			
Test time = 10 min			

4 Conclusions

Nichrome is successfully coated on DSS 2205 by the Detonation Gun technique. The following conclusions are drawn from the investigation of the specimen's erosion behavior.

- The primary reason for pipeline failures appears to be the erosion issue. Metallic pipeline failure is common, yet even with cutting-edge erosion prevention technology, it is still totally unpredictable. Therefore, the first step in choosing the most effective protection and control method is to comprehend and identify the causes of failure.
- Adequate coatings can protect the pipeline surface and serve as the first line of defense against erosion. The effective prevention of erosion was demonstrated by the suitable choice of pipe material and coating.
- To prevent erosion issues, pipelines should be designed with the specific flow parameters such as resistance to higher impact angle, lower flow velocity and lower impact duration.
- Taguchi and ANOVA analysis determined the significance of controlling each parameter for erosion control: velocity (3.2%), erodent discharge (3.78%), angle of impact (7.6%), and time (85.38%).
- As the error fits within the tolerance level (3.03%), it appears that the predicted model can estimate the erosion rate, indicating that it is reliable.
- Thus the effective ways for mitigating and controlling erosion include material pipe selection, coating material, methods, and flow control.

5 Research gaps and future directions

- The literature on internal erosion protection and control methods for metallic pipelines is still very limited. By offering some insights and future perspectives on metallic pipeline protection and control techniques, this research aims to close this research gap.
- Though all of the earlier methods of control and prevention can help reduce erosion, they are not able to prevent it entirely. Therefore, cutting-edge and useful anti-eroding

coating materials and processes, especially in harsh settings, are considered hot development study areas.

- Despite the thermal spray method of nickel–chromium coating being more effective and can safeguard the pipe surface, it is not 100% effective over time and is susceptible to flaws and delamination. To extend their service life, smart materials and methods for pipeline detection, cleaning, and monitoring are therefore going to be required in the future. Another area of active development study is innovative approaches for identifying and avoiding erosion damage.
- Better coatings on pipes over time can increase their lifespan and make pipeline upgrades substantially more affordable. To obtain both technical and financial benefits, a trade-off between erosion prevention and control strategies is therefore inevitable.

Funding The work received no internal/external funding.

Data availability statement The data supporting the findings of this study are available within the manuscript.

Declarations

Conflicts of interests There is not any actual or potential conflict of interest.

References

1. Seghier, M.E.A.B., Höche, D., Zheludkevich, M.: Prediction of the internal corrosion rate for oil and gas pipeline: implementation of ensemble learning techniques. *J. Nat. Gas. Sci. Eng.* **99**, 104425 (2022)
2. Liao, Q., Liang, Y., Tu, R., Huang, L., Zheng, J., Wang, G., Zhang, H.: Innovations of carbon-neutral petroleum pipeline: a review. *Energy Rep.* **8**, 13114–13128 (2022)
3. Peng, S., Zhang, Z., Liu, E., Liu, W., Qiao, W.: A new hybrid algorithm model for prediction of internal corrosion rate of multiphase pipeline. *J. Nat. Gas Sci. Eng.* **85**, 103716 (2021)
4. Wu, T., Chen, Y., Deng, Z., Shen, L., Xie, Z., Liu, Y., Zhu, S., Liu, C., Li, Y.: Oil pipeline leakage monitoring developments in China. *J. Pipeline Sci. Eng.* 100129 (2023)
5. Lu, H., Ma, X., Huang, K., Azimi, M.: Carbon trading volume and price forecasting in China using multiple machine learning models. *J. Clean. Prod.* **249**, 119386 (2020)
6. Yin, H., Liu, C., Wu, W., Song, K., Dan, Y., Cheng, G.: An integrated framework for criticality evaluation of oil and gas pipelines based on fuzzy logic inference and machine learning. *J. Natural Gas Sci. Eng.* **96**, 104264 (2021)
7. Wee, S.K., Yap, Y.J.: CFD study of sand erosion in pipeline. *J. Petrol. Sci. Eng.* **176**, 269–278 (2019)
8. Wang, Q., Ba, X., Huang, Q., Wang, N., Wen, Y., Zhang, Z., Sun, X., Yang, L., Zhang, J.: Modeling erosion process in elbows of petroleum pipelines using large eddy simulation. *J. Petrol. Sci. Eng.* **211**, 110216 (2022)
9. Singh, R., Kumar, S., Gehlot, A., Pachauri, R.: An imperative role of sun trackers in photovoltaic technology: a review. *Renew. Sustain. Energy Rev.* **82**, 3263–3278 (2018)

10. Nguyen, Q.B., Lim, C.Y.H., Nguyen, V.B., Wan, Y.M., Nai, B., Zhang, Y.W., Gupta, M.: Slurry erosion characteristics and erosion mechanisms of stainless steel. *Tribol. Int.* **79**, 1–7 (2014)
11. Krella, A., Marchewicz, A.: Effect of mechanical properties of CrN/CrCN coatings and uncoated 1.402 stainless steel on the evolution of degradation and surface roughness in cavitation erosion. *Tribol. Int.* **177**, 107991 (2023)
12. Heymann, F.J.: A survey of clues to the relation between erosion rate and impact parameters. In: Second rain erosion conference, 2, pp. 683–760 (1967)
13. Zhou, H., Liu, Z., Kikuchi, S., Shibamura, K.: Analysis of fatigue performance of austenitic stainless steels with bimodal harmonic structures based on multiscale model simulations. *Mater. Des.* **226**, 111657 (2023)
14. Solomon, H.D., Devine Jr, T.M.: Duplex stainless steels: a tale of two phases. In: Duplex Stainless Steels, 693–756 (1982)
15. Charles, J.: Structure and properties. In: Proceedings of Conference Duplex Stainless Steels' **91**, 3–48 (1991)
16. Francis, R., Byrne, G.: Duplex stainless steels—alloys for the 21st century. *Metals* **11**(5), 836 (2021)
17. Francis, R.: The corrosion of duplex stainless steels: a practical guide for engineers (2018)
18. Tavana, S.M., Hojjati, M., Liberati, A.C., Moreau, C.: Erosion resistance enhancement of polymeric composites with air plasma sprayed coatings. *Surf. Coat. Technol.* **455**, 129211 (2023)
19. Okokpujie, I.P., Tartibu, L.K., Musa-Basheer, H.O., Adeoye, A.O.M.: Effect of coatings on mechanical, corrosion and tribological properties of industrial materials: a comprehensive review. *J. Bio-and Tribo-Corros.* **10**(1), 2 (2024)
20. Santa, J.F., Espitia, L.A., Blanco, J.A., Romo, S.A., Toro, A.: Slurry and cavitation erosion resistance of thermal spray coatings. *Wear* **267**(1–4), 160–167 (2009)
21. Di, G.G., Brentari, A., Blasi, C., Serra, E.: Microstructure and mechanical properties of plasma sprayed alumina based coatings. *Ceram. Int.* **40**(8), 12861–12879 (2014)
22. Fotovvati, B., Namdari, N., Dehghanghadikolaei, A.: On coating techniques for surface protection: a review. *J. Manuf. Mater. Process.* **3**(1), 1–22 (2019)
23. Kamal, S., Jayaganthan, R., Prakash, S., Kumar, S.: Hot corrosion behavior of detonation gun sprayed Cr₃C₂–NiCr coatings on Ni and Fe-based super alloys in Na₂SO₄–60% V₂O₅ environment at 900 C. *J. Alloy. Compd.* **463**(1–2), 358–372 (2008)
24. Bolelli, G., Colella, A., Lusvardi, L., Puddu, P., Rigon, R., Sasatelli, P., Testa, V.: Properties of HVOF-sprayed TiC-FeCrAl coatings. *Wear* **418**, 36–51 (2019)
25. Kilic, M., Ozkan, D., Gok, M.S., Karaoglanli, A.C.: Room-and high temperature wear resistance of MCrAlY coatings deposited by detonation gun (D-gun) and supersonic plasma spraying (SSPS) techniques. *Coatings* **10**(11), 1107 (2020)
26. Swaminathan, S., Hong, S.M., Kumar, M., Jung, W.S., Kim, D.I., Singh, H., Choi, I.S.: Microstructural evolution and high temperature oxidation characteristics of cold sprayed Ni-20Cr nanostructured alloy coating. *Surf. Coat. Technol.* **362**, 333–344 (2019)
27. Li, Y.J., Dong, T.S., Fu, B.G., Li, G.L., Liu, Q.: Study of the microstructure and properties of cold sprayed NiCr coating. *J. Mater. Eng. Perform.* **30**(12), 9067–9077 (2021)
28. Kawahara, Y.: Development and application of high-temperature corrosion-resistant materials and coatings for advanced waste-to-energy plants. *Mater. High Temp.* **14**(3), 261–268 (1997)
29. Behera, N., Medabalimi, S., Ramesh, M.R.: Effect of impact angles and temperatures on the solid particle erosion behavior of HVOF sprayed WC-Co/NiCr/Mo and Cr₃C₂-CoNiCrAlY coatings. *J. Therm. Spray Technol.*, pp. 1–15 (2023)
30. Abyazi, A., Takht Kiyani, M.: Solid particle erosion wear characteristics of WC-reinforced ni-based coating deposited by oxy-acetylene flame welding. *J. Therm. Spray Technol.*, pp. 1–18 (2023)
31. Davis, J.R. ed.: *Surface Engineering for Corrosion and Wear Resistance*. ASM International (2001)
32. Hutchings, I., Shipway, P.: *Tribology: Friction and Wear of Engineering Materials*. Butterworth-Heinemann (2017)
33. Davis, J.R. ed.: *Nickel, Cobalt, and their Alloys*. ASM International (2000)
34. Zhao, X., Cao, X., Zhang, J., Cao, H., Xie, Z., Xiong, N.: Numerical investigation and dimensionless erosion laws of solid particle erosion in plugged tees. *Powder Technol.* **402**, 117342 (2022)
35. Kuruvila, R., Kumaran, S.T., Khan, M.A., Uthayakumar, M.: Optimization of solid particle erosion of 2205 duplex stainless steel under air jet using Taguchi method. In IOP conference series: materials science and engineering (Vol. 1057, No. 1, p. 012073). IOP Publishing (2021)
36. Sun, Y., Babaian-Kibala, E., Hernandez, S., Martin, J.W. and Alvarez, J.: Design and operations guidelines to avoid erosion problems in oil and gas production systems—one operator's approach. In: NACE CORROSION (pp. NACE-06592). NACE (2006)
37. Alqallaf, J., Teixeira, J.A.: Numerical study of effects of solid particle erosion on compressor and engine performance. *Results Eng.* **15**, 100462 (2022)
38. Fu, Y., Hu, Y., Hu, C., Li, F., Li, C.: Erosion characteristics of molten aluminum droplets bouncing off solid walls in solid rocket motors. *Acta Astronaut.* **201**, 431–444 (2022)
39. Islam, M.A., Farhat, Z.N.: Effect of impact angle and velocity on erosion of API X42 pipeline steel under high abrasive feed rate. *Wear* **311**(1–2), 180–190 (2014)
40. Lopez, D., Congote, J.P., Cano, J.R., Toro, A., Tschiptschin, A.P.: Effect of particle velocity and impact angle on the corrosion-erosion of AISI 304 and AISI 420 stainless steels. *Wear* **259**(1–6), 118–124 (2005)
41. Singh, R., Tiwari, S.A., Mishra, S.K.: Cavitation erosion in hydraulic turbine components and mitigation by coatings: current status and future needs. *J. Mater. Eng. Perform.* **21**, 1539–1551 (2012)
42. Okonkwo, P.C., Mohamed, A.M.: Erosion-corrosion in oil and gas industry: a review. *Int. J. Metall. Mater. Sci. Eng.* **4**(3), 7–28 (2014)
43. Levy, A.V., Chik, P.: The effects of erodent composition and shape on the erosion of steel. *Wear* **89**(2), 151–162 (1983)
44. Lynn, R.S., Wong, K.K., Clark, H.M.: On the particle size effect in slurry erosion. *Wear* **149**(1–2), 55–71 (1991)
45. Clark, H.M., Hartwich, R.B.: A re-examination of the 'particle size effect' in slurry erosion. *Wear* **248**(1–2), 147–161 (2001)
46. Turenne, S., Fiset, M., Masounave, J.: The effect of sand concentration on the erosion of materials by a slurry jet. *Wear* **133**(1), 95–106 (1989)
47. Tewari, U.S., Harsha, A.P., Häger, A.M., Friedrich, K.: Solid particle erosion of carbon fibre- and glass fibre-epoxy composites. *Compos. Sci. Technol.* **63**(3–4), 549–557 (2003)
48. Balamurugan, K., Shanmugam, V., Palani, G., Sundarakannan, R., Sathish, T., Linul, E., Khan, S.A., Asif, M.: Effect of TiC/RHA on solid particle erosion of Al6061 hybrid composites fabricated through a 2-step ultrasonic-assisted stir casting process. *J. Market. Res.* **25**, 4888–4900 (2023)
49. Kuruvila, R., Kumaran, S.T., Uthayakumar, M., Khan, M.A., Ahmed, F.: Erosion behavior of plasma and D-Gun sprayed nichrome coatings on 2205 duplex stainless steel. *Int. J. Interact. Des. Manuf.*, pp. 1–15 (2023)
50. Kuruvila, R., Kumaran, S.T., Khan, M.A.: Solid particle erosion behavior of nichrome coated duplex stainless steel. *Int. J. Adv. Technol. Eng. Explor.* **9**(97), 1741 (2022)

51. Kuruvila, R., Sundaresan, T.K., Ahmed, F., Marimuthu, U.: Electrochemical corrosion behavior of thermally sprayed nichrome coating on duplex stainless steel. *J. Test. Eval.* **52**(1) (2024)
52. Benterki, S., Faci, A., Barka, B. and Rouabah, F., 2023. Evaluation and optimization of erosion parameters' effects on polymeric glasses using Taguchi method. *J. Mater. Eng. Perform.*, pp. 1–9.
53. Choudhary, M., Sharma, A., Agarwal, P., Bhardwaj, A., Patnaik, A.: Optimization of solid particle erosion behaviour of waste marble dust filled glass fiber polymer composite using Taguchi approach. *Mater. Today: Proc.* **44**, 4908–4912 (2021)
54. Kuruvila, R., Kumaran, S.T., Khan, M.A.: Optimization of erosion-corrosion behavior of nichrome coated 2205 duplex stainless steel using grey relational analysis. *Surf. Rev. Lett.* **29**(07), 2250087 (2022)
55. Sundararajan, G., Prasad, K.U.M., Rao, D.S., Joshi, S.V.: A comparative study of tribological behavior of plasma and D-gun sprayed coatings under different wear modes. *J. Mater. Eng. Perform.* **7**, 343–351 (1998)
56. Wood, R.J.K., Speyer, A.J.: Erosion–corrosion of candidate HVOF aluminium-based marine coatings. *Wear* **256**(5), 545–556 (2004)
57. Panakarajupally, R.P., Mirza, F., El Rassi, J., Morscher, G.N., Abdi, F., Choi, S.: Solid particle erosion behavior of melt-infiltrated SiC/SiC ceramic matrix composites (CMCs) in a simulated turbine engine environment. *Compos. B Eng.* **216**, 108860 (2021)
58. Sathish, T., Chandramohan, D., Vijayan, V., Sebastian, P.J.: Investigation on microstructural and mechanical properties of Cu reinforced with Sic composites prepared by microwave sintering process. *J. New Mater. Electrochem. Syst.* **22**(1), 5–9 (2019)
59. Nagaraja, S., Nagegowda, K.U., Kumar V, A., Alamri, S., Afzal, A., Thakur, D., Kaladgi, A.R., Panchal, S., Saleel C.A.: Influence of the fly ash material inoculants on the tensile and impact characteristics of the aluminum AA 5083/7.5 SiC composites. *Materials*, **14**(9), 2452 (2021)
60. Al-Bukhaiti, M.A., Ahmed, S.M., Badran, F.M.F., Emara, K.M.: Effect of impingement angle on slurry erosion behaviour and mechanisms of 1017 steel and high-chromium white cast iron. *Wear* **262**(9–10), 1187–1198 (2007)
61. Yang, S., Fan, J., Zhao, S., Dai, S., Han, L., Wang, J., Yang, S., Zhang, L., Li, J.: Experimental study on erosion behavior of fracturing pipelines involving fluctuating stress. *Wear* **518**, 204626 (2023)
62. Blach, J., Falat, L., Ševc, P.: Fracture characteristics of thermally exposed 9Cr–1Mo steel after tensile and impact testing at room temperature. *Eng. Fail. Anal.* **16**(5), 1397–1403 (2009)
63. Singh, J., Kumar, S., Mohapatra, S.K.: Study on solid particle erosion of pump materials by fly ash slurry using Taguchi's orthogonal array. *Tribologia-Finnish J. Tribol.* **38**(3–4), 31–38 (2021)
64. Kiragi, V.R., Patnaik, A., Singh, T., Fekete, G.: Parametric optimization of erosive wear response of TiAlN-coated aluminium alloy using Taguchi method. *J. Mater. Eng. Perform.* **28**, 838–851 (2019)
65. Gunaraj, V., Murugan, N.: Application of response surface methodology for predicting weld bead quality in submerged arc welding of pipes. *J. Mater. Process. Technol.* **88**(1–3), 266–275 (1999)
66. Srinivasan, R., Pridhar, T., Ramprasath, L.S., Charan, N.S., Ruban, W.: Prediction of tensile strength in FDM printed ABS parts using response surface methodology (RSM). *Mater. Today: Proc.* **27**, 1827–1832 (2020)

Publisher's Note Springer Nature remains neutral with regard to jurisdictional claims in published maps and institutional affiliations.

Springer Nature or its licensor (e.g. a society or other partner) holds exclusive rights to this article under a publishing agreement with the author(s) or other rightsholder(s); author self-archiving of the accepted manuscript version of this article is solely governed by the terms of such publishing agreement and applicable law.